RSC Advances

Hydration of the Sulfuric Acid-Oxalic Acid Complex: Acid Dissociation and Its Atmospheric Implication

Shou-Kui Miao,[1] Shuai Jiang,[1] Jiao Chen,[1] Yan Ma,[1] Yu-Peng Zhu,[1] Yang Wen,[1] Miao-Miao Zhang,[1,2] and Wei Huang[1,2]*

[1]*Laboratory of Atmospheric Physico-Chemistry, Anhui Institute of Optics & Fine Mechanics, Chinese Academy of Sciences, Hefei, Anhui 230031, China*

[2]*School of Environmental Science & Optoelectronic Technology, University of Science and Technology of China, Hefei, Anhui 230026, China*

*E-mail: huangwei6@ustc.edu.cn

Abstract

Oxalic acid (OA), one of the most common organic acids in the Earth's atmosphere, is expected to enhance the nucleation and growth of nanoparticles containing sulfuric acid (SA) and water (W); however, the details about the hydration of OA-SA are poorly understood, especially for the larger clusters with more water molecules. We have investigated the structural characteristics and thermodynamics of these clusters using density functional theory at the PW91PW91/6-311++G(3df, 3pd) level. The favorable free energies of formation and obvious concentrations of the OA-SA-W_n(n=0-6) clusters at 298.15 K predict that oxalic acid can contribute to the aerosol nucleation process by binding to sulfuric acid and water until n=6. There is strong temperature dependence for the complexes formation, and the energy order of these complexes is altered from 100 to 400 K, regardless of different cluster sizes or different isomers within the same cluster size. The lower temperature and higher relative humidity promote the formation of hydrates. Additionally, the investigation of acid dissociation predicts that several acid-dissociated models could coexist in the

atmosphere, specifically when more water molecules are present. Fewer waters may be needed to cause the acid dissociation, as the relative acidity of the cluster increases, which plays a key role in forming relatively stable hydrated clusters of OA-SA. Finally, the Rayleigh scattering properties of OA-SA-W_n(n=0-6) has been systematically investigated for the first time to furthermore discuss its atmospheric implication.

1. INTRODUCTION

New particle formation (NPF), which is frequently observed in the atmosphere, is an important source of atmospheric aerosols, which play a significant effect on humankind via their influence on weather, climate and health quality.[1-4] Although nucleation phenomena have been constantly investigated in the past, the nucleation mechanisms and the species involved in the atmospheric nucleation are still highly uncertain.[2, 5-8] Sulfuric acid (SA) has been proved as the critical aerosol nucleation precursor by numerous atmospheric observations and laboratory studies,[5, 9, 10] however, the concentrations of sulfuric acid in the range of 10^5-10^7 cm^{-3} are not sufficient to explain the measured nucleation rates in the actual atmospheric environment, predicting that other ternary species are involved in the nucleation phenomena.[11-14] Recently, the importance of organic species in aerosol nucleation has been recognized.[6, 15-18]

Atmospheric observations have revealed that the aerosols often contain a large number of organic carbonyls and acids, which may participate in nucleation and growth to form nanoparticles.[19-23] Recent researches also showed that some organic

aids including benzoic, p-toluic and m-toluic acids, can be considered as catalysts to enhance the nucleation of sulfuric acid and water via the formation of strongly hydration-bound clusters.[16-18, 24, 25] Dicarboxylic acids represent the common organic acids and are expected to partition to the condensed phase because of its relatively lower vapor pressure.[26, 27] Xu and Zhang indicated that dicarboxylic acids can contribute to aerosol formation by binding to sulfuric acid and ammonia.[28]

In this work, oxalic acid (OA), which is the most prevalent dicarboxylic acid in the atmosphere and a major constituent of aerosol particles,[27, 29, 30] is selected to discuss its role in the cluster formation. According to the results of Martinelango *et al.*,[30] the gas-phase concentrations of oxalic acid are in the $9.3 \times 10^{10} - 5.4 \times 10^{12}$ cm^{-3} range with mean and median values of 4.9×10^{11} cm^{-3} and 3.9×10^{11} cm^{-3}, respectively. This means that typical concentrations of OA are 10^2-10^3 times higher than those of ammonia.[31] It has recently been found that OA is effective at binding with NH$_3$, an important nucleating species in the atmosphere, to form thermodynamically stable clusters which should be found in appreciably significant concentrations in the atmosphere.[32] Using the Density Functional Theory (DFT), Xu *et al.* pointed out that oxalic acid can catalyse the production of positively charged prenucleation clusters, showing its role in nucleation of positive ions in the Earth's atmosphere.[33]

Shortly, oxalic acid, one of the most common organic acids in the Earth's atmosphere, is expected to enhance nucleation and growth of nanoparticles. However, the details about the hydration of oxalic acid with sulfuric acid, the dominant atmospheric nucleation precursor, are poorly understood, especially for the larger

clusters with more water molecules. Herein, the hydration of OA-SA is studied using density functional theory (DFT) at the PW91PW91/6-311++G(3df,3pd) level. We searched for the minima energy structures of OA-SA-W_n(n=0-6) and determined the thermodynamic properties of these clusters. We used these results to gain further insight into the ternary nucleation of sulfuric acid, oxalic acid and water, as well as the nature of acid dissociation at a molecular level. The effects of temperature on the formation of OA-SA-W_n(n=0-6) and its atmospheric relevance are studied. In addition, the Rayleigh scattering properties of the hydrates are investigated for the first time. This work is a continuation of longstanding efforts to investigate ion-molecule interactions, hydrogen-bonded interactions, water cluster formation and atmospheric processes.[34]

2. THEORETICAL METHODS

The initial geometries of the monomers and OA-SA-W_n(n=0-6) clusters were obtained with the Basin-Hopping (BH) algorithm coupled with DFT. Generalized gradient approximation in the Perdew-Burke-Ernzerhof (PBE) functional and the double numerical plus d-functions (DND) basis set, implemented in DMol[3],[35, 36] were used to optimize the structures of this system. This method was highly efficient to explore atomic and molecular systems in our previous studies.[37-42]

For this system, five to fifteen BH searches according to the cluster sizes, which consist of 1000 sampling steps at 3000 K with randomly generated molecular structures, were performed. Then, the results were first optimized at the PW91PW91/6-31+G* level by DFT. The stable isomers from the first optimization

were selected and further optimized by the PW91PW91/6-311++G(3df,3pd) level of theory to get the final configurations. This methodology was used because it would take much less time to obtain the final structures with twice optimizations compared to one direct optimization via the PW91PW91/6-311++G(3df,3pd) level of theory. For each stationary point, frequency calculations were performed to make sure that no imaginary frequencies were present and that consequently, the structure of interest represented a local or a global minimum on the potential energy surface. The convergence criteria were default setting in the Gaussian 09 suite of programs.[43]

Finally, the optimized geometries were used in single point energy calculations with the DF-MP2-F12 (second-order Møller-Plesset perturbation theory-explicitly correlated methods with density fitting) method implemented in Molpro 2010.1.[44] We combined the PW91PW91/6-311++G(3df,3pd) thermodynamic corrections with DF-MP2-F12 single point energies to evaluate the Zero-point corrected energies [E(0 K)], energies including atmospheric temperature enthalpies [H(T)] and Gibbs free energies [G(T)]. PW91PW91 functional was chosen to be the specific DFT methods in this study, because of its fine performance on a large number of atmospheric clusters containing sulfuric, water and the common organic acids, including predictions of structural characteristics, the thermodynamics of cluster formation and satisfactory similarity compared with experimental results.[28, 33, 45, 46]

Based on the global minima of OA-SA-W_n(n=0-6) obtained in this work, we have evaluated the Rayleigh scattering intensities and polarization ratios of the prenucleation clusters. The binding mean isotropic and anisotropic polarizabilities of

the clusters were calculated at CAM-B3LYP/aug-cc-pVDZ level of theory. The

benchmark work of small clusters containing SA, W and OA was performed by the

earlier studies.[47-50] On the basis of the analysis, they found that

CAM-B3LYP/aug-cc-pVDZ was a good compromise between efficiency and

accuracy yielding good agreement with both experimental and CCSD(T) values of the

polarizability. Light scattering intensities and the isotropic mean polarizabilities $\bar{\alpha}$

as well as anisotropic polarizabilities $\Delta\alpha$ and the relevant computation methods,

have been given in our earlier study.[49]

3. RESULTS AND DISCUSSION

3.1 Structures

Figure 1 displays the optimized structures of the global and some special local

minima at the PW91PW91/6-311++G(3df,3pd) level of theory for OA-SA-W_n(n=0-6)

that would be discussed in this part, more local minima could be found in the

electronic supplementary information (Figures S1-S7). The representations of these

structures are defined using ni(x) notation. In this notation, "n" (n = 0 - 6) represents

the number of water molecules. "i" (i = a - t), displayed in order of increasing

electronic energy at 0 K for each cluster size, denotes the different isomers with the

same value of n. The index "x"(x = N, SA, OA, SA&OA) is utilized to distinguish

different acid-dissociated models of the clusters. The structures are labeled "N" if the

clusters remain neutral as OA-SA-W_n, "SA" if only sulfuric acid undergoes acid

dissociation to form di-ionic OA-SA^--W^+-W_{n-1} clusters, "OA" if only oxalic acid

undergoes acid dissociation to form di-ionic OA^--SA-W^+-W_{n-1} clusters, and

"SA&OA" if both acids undergo their first acid dissociation to form tetra-ionic $OA^--SA^--(W^+)_2-W_{n-2}$ clusters.

In Figure 1, for the OA-SA-W complexes, the 1a(N) isomer, which is based on the 0a(N) dimer with water bound to the remaining free hydroxyl group and an oxygen atom, is the most stable in terms of E(0 K) and G(298.15 K). In the most stable isomer 2a(N) of OA-SA-W_2, the W_2 dimer binds the sulfuric acid monomer with one strong (1.441 Å) and one weak (1.814 Å) hydrogen bonds, which are both stronger than those in isomer 1a(N) (1.599 Å and 2.126 Å, respectively). Di-ionic structures 2d(OA) and 2i(SA) are found in the lowest energy isomers, illustrating that the deprotonation of acid molecules can begin even when only two water molecules are added. For the OA-SA-W_3 clusters, the most stable structure is clearly di-ionic isomer 3a(SA) of deprotonated sulfuric acid forming SA^- and W^+ ions, where the hydronium and waters bridge SA^- and OA with a network of six hydrogen bonds. Unlike neutral structures 3i(N) and 3j(N) where the waters are equally likely to form bridging or outer hydrogen bonds, the hydronium in the di-ionic isomer favors the formation of bridging structures where the hydronium ion donates three hydrogen bonds.

For the OA-SA-W_4 hydrates, 4a(SA) and 4b(SA) are the most stable structures in terms of E(0 K) and G(298.15 K), respectively. We also found one di-ionic isomer 4c(OA) of deprotonated oxalic acid and one tetra-ionic isomer 4k(SA&OA). The tetra-ionic structure 4k(SA&OA), although much higher in energy than the minima, suggests a new structural motif that emerges as more waters are added. In the clusters OA-SA-W_5, the lowest electronic energy structure at 0 K is isomer 5a(SA), which

resembles structure 4a(SA) of OA-SA-W$_4$ but with a fifth water inserted into the stable square. Structure 5b(SA), however, is the global minima in terms of G(298.15 K), and this structure consists of the OA-SA$^-$ dimer structure with four waters and one hydronium acting as hydrogen bond acceptors on one side of the OA-SA$^-$ dimer. For the system of OA-SA-W$_6$, the most stable structure 6a(SA) forms a strong and stable quasi-cubic configuration through five waters, one hydronium and one sulfuric acid molecule, and there is no other isomer within 1 kcal mol^{-1}. Moreover, the values of electronic energy change ΔE and free energy change ΔG in Table 1 show that the OA-SA-W$_6$ hydrates are more stable than the OA-SA-W$_5$ clusters, and more favorable than the OA-SA-W$_4$ and OA-SA-W$_5$ clusters.

3.2 Acid Dissociation

The nature of acids in an aqueous environment is fundamental to many aspects of chemistry. The defining feature of an acid is its ability to transfer a proton to water, i.e., acid dissociation, which is a significant topic and has attracted the attention of many researchers.[51-55] Therefore, in this work, we paid close attention to the dissociation of hydrated sulfuric acid compounded with oxalic acid. The data in Table 1 as well as Tables S1-S4 are used to predict the picture of the acid dissociation for the OA-SA-W$_n$(n=0-6) complexes in terms of E(0 K) and G(298.15 K).

In Figure 2, at 0 K, a cluster of an OA-SA dimer and a single water remain undissociated. The first deprotonation of sulfuric acid or oxalic acid emerges once the second water is added to the OA-SA-W trimer, but the completely neutral moieties appear more stable in the top of Figure 2. However, the addition of a third water

results in the deprotonation of sulfuric acid for most of the clusters, with the ionic species more stable than the completely neutral moieties. Upon the addition of a fourth water molecule, the sulfuric and oxalic acids dissociate simultaneously. For the OA-SA-W_4 clusters, the di-ionic cluster of deprotonated sulfuric acid is 0.89 kcal mol^{-1} more stable than the di-ionic cluster of deprotonated oxalic acid, which is 2.81 kcal mol^{-1} more stable than the tetra-ionic cluster. The stabilities of the di-ionic cluster of deprotonated oxalic acid and the tetra-ionic clusters are close to the di-ionic species of deprotonated sulfuric acid after five waters have been added to the clusters, as shown in the top of Figure 2. In OA-SA-W_5, the differences in several types of ionic clusters are less than 0.2 kcal mol^{-1} in terms of E(0 K). Among the isomers of OA-SA-W_6, the tetra-ionic cluster 6c(SA&OA) is slightly less stable than the global minima 6a(SA). We also found that the ionic species are more stable and favorable than the neutral clusters with more than two waters bound to the clusters. This indicates that acid dissociation events exist in the formation of OA-SA-W_n clusters and play a role in the stability of this system.

The bottom of Figure 2 indicates that the di-ionic cluster of deprotonated sulfuric acid is favorable for n = 2 - 6 at 298.15 K, while the ionic clusters of deprotonated oxalic acid, regardless of whether sulfuric acid is simultaneously dissociated or not, have unfavorable thermodynamics. However, this does not imply that the ionic clusters with oxalic acid dissociation would never form but instead that there would be a much smaller number of these clusters at equilibrium compared to those with the di-ionic cluster of deprotonated sulfuric acid. The exact values depend on the initial

concentrations of water, sulfuric acid and oxalic acid as well as the temperature. Furthermore, the similar stabilities between the di-ionic clusters (including $OA\text{-}SA^-\text{-}W^+\text{-}W_{n-1}$ and $OA^-\text{-}SA\text{-}W^+\text{-}W_{n-1}$) and the tetra-ionic clusters $(OA^-\text{-}SA^-\text{-}(W^+)_2\text{-}W_{n-2})$ for n = 5 - 6 also predict that these three acid-dissociated models could coexist in the atmosphere, especially when more water molecules are present.

Additionally, according to earlier research on the $SA\text{-}W_n(n=1-6)$ system, ionic $SA^-\text{-}W^+\text{-}W_{n-1}$ clusters are less stable than neutral $SA\text{-}W_n$ clusters for n ≤ 3 and become the global minima in terms of E(0 K) and G(298.15 K) when n ≥ 4 and n=6, respectively.[56] For the $OA\text{-}W_n(n=1-6)$ hydrates, oxalic acid dissociates until n ≥ 5, and only three are found to ionize with many of the neutral clusters which are found to have greater stability, indicating the propensity of oxalic acid to form highly stable neutral clusters with water.[44] However, according to our study of the $OA\text{-}SA\text{-}W_n(n=0-6)$ clusters, the finding the ionic clusters are more stable than neutral clusters for n ≥ 3 both in terms of E (0 K) and G (298.15 K) could predict that the additional SA or OA can promote acid dissociation of the hydrates and that fewer waters may be needed to cause the acid dissociation, as the relative acidity of a cluster increases with more acid molecules (SA and OA here).

3.3 Temperature Dependence of Clusters Formation

In previous studies, people revealed that the thermodynamical properties of clusters depended on the various temperatures, and supported that temperature effects contributed to the clusters formation, which should be important for understanding a

nucleation mechanism.[49, 57-59] However, because the wall losses of the complexes increases as the temperature lowers, it is hard to fulfill the relevant experiments at the low temperature.[60, 61] With quantum chemistry calculations, we can get such data, and the following results may aid in predicting the effect of temperature on the formation of OA-SA-W_n(n=1-6).

The change in Gibbs free energy with temperatures from 100 to 400 K could have a large influence on the relative populations of different isomers; thus, an effect of temperature on the relative populations of isomers for OA-SA-W_n(n=1-6) is expected. Here we have calculated their relative populations at various temperatures:

$$p_i = \exp(-\Delta\Delta G_i / RT) / \sum_i \exp(-\Delta\Delta G_i / RT) \tag{1}$$

where p_i is the relative population of the ith isomer at one cluster size, $\Delta\Delta G_i$ is the Gibbs free energy of the ith isomer compared to the most stable one, R is the ideal gas constant, and T is the temperature.[62]

For n = 1 in Figure 3(a), although their relative populations decrease quickly while those of other local minima increase with increasing temperature, the most stable structures 1(a-c)(N) remain more predominant than the other low-energy isomers until 400 K, which occurs similarly with n = 2 and n = 6 (Figure 3(b) and Figure 3(f), respectively). However, for n = 3 as shown in Figure 3(c), the global minima 3a(SA) is more prevalent than any other minima below T = 350 K, but its predominance decreases thereafter. At temperatures above 350 K, the two isomers 3i(N) and 3j(N) compete for the global minima. For n = 4, as seen in Figure 3(d), the conformational population of isomer 4b(SA) increases as the temperature increases

and is more prevalent than 4a(SA) at approximately $T = 150$ K but then decreases above 200 K, which is its turning point. Meanwhile, the conformational population of isomer 4e(SA) increases from 100 to 400 K and exceeds the other local minima at about $T = 350$ K. For n = 5 (Figure 3(e)), isomer 5b(SA) has a greater proportion than the other isomers where their conformational populations increase or decrease in a relatively small range across the temperature values.

In conclusion, as the temperature increases, the weight of the global minima decreases while that of other local minima increases. The effects of temperature could contribute to the alternation of the stability order of the isomers, but the patterns for the OA-SA-W_n(n=1-6) system are significantly different with various water molecules due to their considerably different Gibbs free energy values among the stable minima, which also reflects the different flatness of their potential energy surfaces.[49]

Meanwhile, the stepwise Boltzmann averaged binding free energy (ΔG_n) values for the formation of hydrates at $T = 100$ - 400 K are shown in Figure 4, which illustrates that binding decreases from 100 to 400 K for each cluster size, *i.e.* the clusters are less favorable at higher temperatures. There is a strong temperature dependence for the OA-SA-W_n(n=1-6) cluster formation; the lowest free energy shifts from n = 3 at $T = 100$ K to n = 1 around $T = 150$ K. And then, the tetrahydrate and the hexahydrate alter their free energy order from $T = 150$ to 200 K. At $T = 250$ - 400 K, the order of the first four lowest free energy values is n = 1, 2, 3, 6. The size of n = 6 are more favorable than the size of n = 4 and 5 because of the formation of a stable

cubic structure. The pentahydrate is the least stable cluster up to T = 250 K, but replaced by the tetrahydrate at T ≥ 300 K. Besides, Figure 4 demonstrates that the free energy of association of water with OA-SA dimer is favorable up to size n = 6 at T = 100 K - 300 K, but not at higher temperatures. At T = 350 K, only clusters of size n = 1 have favorable thermodynamics. According to Kim *et al.*,[57] it is easy to change the stabilities of the clusters containing multiple hydrogen bonds when the temperature rises, which is a result of the entropy effect and may explain the phenomenon of a strong temperature dependence for OA-SA-W_n(n=1-6) binding with a large number of hydrogen bonds.

3.4 Atmospheric Relevance

The free energy of formation of the heterodimer cluster OA-SA at 298.15 K (-5.38 kcal mol^{-1} in Table 1) suggests that oxalic acid can contribute to the aerosol nucleation process by effectively binding to sulfuric acid, the dominant nucleating species in the atmosphere. It is very significant to find the actual concentration of the heterodimer cluster to investigate its effect in the realistic atmospheric condition. To estimate the actual concentration of oxalic acid - sulfuric acid cluster an approach followed is performed.[44] From the Boltzmann averaged binding free energy ΔG(298.15 K), the equilibrium constant K for the formation of the cluster from the respective monomers is given:

$$K = [OA-SA]/\{[OA][SA]\} = \exp(-\Delta G/RT) \qquad (2)$$

The value of the relative population fraction (RPF) is then defined by:

$$RPF = [OA-SA]/[OA] = K[SA] \qquad (3)$$

where the typical and reasonable concentration of oxalic acid [OA] was considered as 5×10^{11} cm^{-3}, and that of sulfuric acid [SA] was 5×10^{7} cm^{-3}.[12, 13, 30] Thus, the OA-SA cluster was calculated to have a concentration of about 10^{4} cm^{-3}. The obvious concentration of the dimer further demonstrates the significance of the OA-SA cluster in the atmosphere. Additionally, for the hydrates, the water molecules could easily bind to the OA-SA core based on the favorable stepwise free energies of formation of the OA-SA-W_n(n=1-6) clusters (Table 1), to promote the aerosol formation process. However, the binding number of water molecules in the clusters could be affected by the various relative humidities (RHs).[63] To get further results, the hydrate distributions of non-aqueous "cores" (oxalic acid - sulfuric acid heterodimer) were estimated at various RHs. As an n-hydrate in this study, its relative concentration is defined by:

$$\rho(1,n)/\rho_{OA-SA}^{total} = \rho(1,n)/[\rho(1,0)+\rho(1,1)+\cdots+\rho(1,6)] = K_1K_2\cdots(S\times P_W^{eq}/P)^n$$

$$/[1+K_1(S\times P_W^{eq}/P)+\cdots+K_1K_2\cdots K_6(S\times P_W^{eq}/P)^6] \qquad (4)$$

with the equilibrium constant K_n for the formation of an n-hydrate from one water molecule and (n-1)-hydrate. Moreover, ρ represents the concentration of different species and S is the saturation ratio, which is defined as the ratio of the proper partial pressure of the water vapor to the saturation vapor pressure P_W^{eq}; thus, relative humidity is defined as RH = 100% $\times$ S, and the reference pressure (P) is 1 atm.[56, 63-65] The hydration level, n, can be any value between 1 and 6.

With the computational method used, we calculated the composition of hydrates as a fraction of the initial OA-SA dimer at 20, 50, 80 and 100% RH with a constant temperature of 298.15 K. As shown in Figure 5, 84% of OA-SA is non-hydrated at

20% RH, but that number decreases to 65% and 51% at 50% RH and 80% RH,

respectively. The most common hydrated clusters are the monohydrates, which

comprise 15 - 39%, followed by the dihydrates (1 - 15%). The trihydrates and

tetrahydrates are virtually nonexistent at 20% RH but form as much as 3% and 0.2%

of these clusters at 100% RH. The larger (n ≥ 5) hydrates form in very low abundance.

The general trend in all cases is more extensive hydration with growing RH.

At the most tropospherically reasonable conditions (relative humidity and

temperature), the total concentration of the OA-SA dimer in these clusters was

dispersed mainly into non-hydrate species and monohydrates. The sensitivity of the

hydrate distributions to relative humidity was obvious, as we previously determined.

The dimer complex of sulfuric and oxalic acids hydrates quite effectively at higher

RH. Nearly 35% - 57% of the clusters are hydrated with the relative humidities

greater than 50%. In the hydration of OA-SA, we found the monohydrate to be the

most prevalent species, and as Table 1 reveals, the monohydrate is more favorable

than the other hydrates.

3.5 Optical Properties

Aerosols, which are formed in the atmosphere via nucleation and growth, effect

the climate by acting as either scatterers or absorbers of incident solar radiation.[1-4]

However, understanding of the impact on the climate from the effects of atmospheric

pre-nucleation clusters on solar radiation is lacking.[49] Therefore, it is very important

to study the optical properties of the clusters. For these clusters, Rayleigh scattering is

the dominant scattering mechanism.[47, 48] In this work, we investigate the polarizability

and Rayleigh light scattering properties of the OA-SA-W_n(n=0-6) clusters for the first time.

From Figure 6(a), we could find that the isotropic mean polarizabilities $\bar{\alpha}$ are quite size dependent and vary linearly with correlation coefficient $\rho = 0.996$, which is consistent with the studies of sulfuric acid hydration systems and methanol clusters.[48,66] In comparison, the change in the anisotropic polarizabilities $\Delta\alpha$ is non-monotonic with the increasing water molecules in Figure 6(b). It is seen that the anisotropic polarizabilities $\Delta\alpha$ show quite a different pattern as from dihydrate to pentahydrate the anisotropic polarizabilities decreases quickly and then increases from pentahydrate to hexahydrate.

In Figure 6(c) and Figure 6(d), the Rayleigh light scattering intensity of natural light $\Re_n$ and the depolarization ratios σ_n of the OA-SA-W_n(n=0-6) clusters can be viewed as a function of the number of water molecules in the cluster. As shown in the results of sulfuric acid hydration systems,[48] the non-linear dependence of $\Re_n$ on the number of water molecules is indicated to follow the trend of a second order polynomial with correlation coefficient $\rho = 0.981$. The calculated depolarization ratios σ_n are observed to quickly decline with the growing cluster size. This is due to the increase of the mean isotropic polarizability with cluster size while the anisotropic polarizability should be relatively constant. This is in accordance with what is to be anticipated as the cluster changes from a molecular cluster into a spherical isotropic particle.[49]

According to the previous research of investigating the relationship between hydrogen bonding number and cluster polarizability,[67] we have fitted the calculated $\bar{\alpha}$ values as a linear function of cluster size n, $\bar{n}_H$:

$$\bar{\alpha} = a + b \times n + c \times \bar{n}_H \qquad (5)$$

where $\bar{n}_H = n_H / n$ represents the average hydrogen bonding number in the clusters. The fit is found to be excellent with a correlation efficient as 0.983, indicating that the hydrogen bonds of the OA-SA-W$_n$(n=0-6) system could contribute to the cluster polarizalibity effectively.

4. CONCLUSION

For the OA-SA-W$_n$(n=0-6) clusters, we have obtained the global and many local minima for each cluster size. We investigated the thermodynamics of sulfuric acid-oxalic acid dimer hydration using DFT calculations and discussed its acid dissociation and implication on atmospheric nucleation. The present study led to these findings:

(1) The results give us a picture of the acid dissociation for the sulfuric acid-oxalic acid dimer hydrates: (1.1) The acid dimer undergoes the deprotonation of one acid molecule after the addition of only two waters and then both acid molecules with four waters added. (1.2) The ionic species is more stable and favorable than the neutral cluster once three water molecules have been added to the cluster, illustrating that acid dissociation events contribute to forming relatively stable large hydrated clusters. (1.3) The stabilities of di-ionic clusters and tetra-ionic clusters are similar with larger hydrates of five and six water molecules, which indicates these

17

acid-dissociated models could coexist with more waters. (1.4) With the addition of sulfuric acid or oxalic acid molecule, fewer waters are required to cause the acid dissociation as the relative acidity of a hydrate increases with more acid molecules, compared to the $OA\text{-}W_n$ and $SA\text{-}W_n$ systems.

(2) Thermodynamics and concentration indicate oxalic acid probably form cluster with sulfuric acid in the atmosphere. The stepwise free energies of formation of the hydrates at 298.15 K are favorable, suggesting that OA can contribute to the nucleation process by binding to SA and W until n=6.

(3) The relative populations of different isomers within the same cluster size at various temperatures from 100 K to 400 K show that the weight of the global minima decreases but that of other local minima competes, *i.e.* the stability order change of isomers. The free energy of association of water with acid dimer is favorable up to size n=6 at T=100-300 K, but not at higher temperatures, and the energy order of different cluster sizes are also altered with different temperatures.

(4) The total concentration of OA-SA in these clusters was dispersed mainly in the non-hydrated and monohydrates. Nearly 35% - 57% of clusters are hydrated when the relative humidities are more than 50%. With higher RH, the number of water molecules in the clusters increases, as expected.

(5) We could find that the Rayleigh scattering intensities of natural light nearly follow the second order polynomial trend with the growing cluster size, and the isotropic mean polarizabilities show linear relation with the number of water molecules in this system.

ACKNOWLEDGEMENTS

References

1. R. J. Charlson, S. Schwartz, J. Hales, R. D. Cess, j. J. COAKLEY, J. Hansen and D. Hofmann, *Science*, 1992, **255**, 423-430.
2. M. Kulmala, *Science*, 2003, **302**, 1000-1001.
3. D. B. Kittelson, W. Watts and J. Johnson, *Atmos. Environ.*, 2004, **38**, 9-19.
4. A. Saxon and D. Diaz-Sanchez, *Nat. Immunol.*, 2005, **6**, 223-226.
5. R. Zhang, A. Khalizov, L. Wang, M. Hu and W. Xu, *Chem. Rev.*, 2011, **112**, 1957-2011.
6. R. Zhang, I. Suh, J. Zhao, D. Zhang, E. C. Fortner, X. Tie, L. T. Molina and M. J. Molina, *Science*, 2004, **304**, 1487-1490.
7. M. Kulmala, J. Kontkanen, H. Junninen, K. Lehtipalo, H. E. Manninen, T. Nieminen, T. Petäjä, M. Sipilä, S. Schobesberger and P. Rantala, *Science*, 2013, **339**, 943-946.
8. M. Kulmala, T. Petäjä, T. Nieminen, M. Sipilä, H. E. Manninen, K. Lehtipalo, M. Dal Maso, P. P. Aalto, H. Junninen and P. Paasonen, *Nat. Protoc.*, 2012, **7**, 1651-1667.
9. B. R. Bzdek, M. R. Pennington and M. V. Johnston, *J. Aerosol Sci.*, 2012, **52**, 109-120.

10. M. Kulmala, H. Vehkamäki, T. Petäjä, M. Dal Maso, A. Lauri, V.-M. Kerminen, W. Birmili and P. H. McMurry, *J. Aerosol Sci.*, 2004, **35**, 143-176.

11. C. Kuang, I. Riipinen, S.-L. Sihto, M. Kulmala, A. McCormick and P. McMurry, *Atmos. Chem. Phys.*, 2010, **10**, 8469-8480.

12. M. Kulmala and V.-M. Kerminen, *Atmos. Res.*, 2008, **90**, 132-150.

13. J. Smith, M. Dunn, T. VanReken, K. Iida, M. Stolzenburg, P. McMurry and L. Huey, *Geophys. Res. Lett.*, 2008, **35**, L04808.

14. P. Paasonen, T. Nieminen, E. Asmi, H. Manninen, T. Petäjä, C. Plass-Dülmer, H. Flentje, W. Birmili, A. Wiedensohler and U. Horrak, *Atmos. Chem. Phys.*, 2010, **10**, 11223-11242.

15. J. Fan, R. Zhang, D. Collins and G. Li, *Geophys. Res. Lett.*, 2006, **33**, L15802.

16. R. Zhang, L. Wang, A. F. Khalizov, J. Zhao, J. Zheng, R. L. McGraw and L. T. Molina, *Proc. Nati. Acad. Sci.*, 2009, **106**, 17650-17654.

17. A. B. Nadykto and F. Yu, *Chem. Phys. Lett.*, 2007, **435**, 14-18.

18. J. Zhao, A. Khalizov, R. Zhang and R. McGraw, *J. Phys. Chem. A*, 2009, **113**, 680-689.

19. J. Zhao, N. P. Levitt and R. Zhang, *Geophys. Res. Lett.*, 2005, **32**, L09802.

20. J. Zhao, N. P. Levitt, R. Zhang and J. Chen, *Environ. Sci. Technol.*, 2006, **40**, 7682-7687.

21. W. Lei and R. Zhang, *J. Phys. Chem. A*, 2001, **105**, 3808-3815.

22. D. Zhang, W. Lei and R. Zhang, *Chem. Phys. Lett.*, 2002, **358**, 171-179.

23. J. Zhao, R. Zhang, K. Misawa and K. Shibuya, *J. Photoch. Photobio. A*, 2005, **176**, 199-207.

24. R. Zhang, *Science*, 2010, **328**, 1366-1367.

25. R. McGraw and R. Zhang, *J. Chem. Phys.*, 2008, **128**, 064508.

26. A. J. Prenni, P. J. DeMott, S. M. Kreidenweis, D. E. Sherman, L. M. Russell and Y. Ming, *J. Phys. Chem. A*, 2001, **105**, 11240-11248.

27. A. Limbeck, H. Puxbaum, L. Otter and M. C. Scholes, *Atmos. Environ.*, 2001, **35**, 1853-1862.

28. W. Xu and R. Zhang, *J. Phys. Chem. A*, 2012, **116**, 4539-4550.

29. A. Chebbi and P. Carlier, *Atmos. Environ.*, 1996, **30**, 4233-4249.

30. P. K. Martinelango, P. K. Dasgupta and R. S. Al-Horr, *Atmos. Environ.*, 2007, **41**, 4258-4269.

31. D. Hanson and F. Eisele, *J. Geophys. Res.*, 2002, **107**(D12), 4158.

32. K. H. Weber, Q. Liu and F.-M. Tao, *J. Phys. Chem. A*, 2014, **118**, 1451-1468.

33. Y. Xu, A. B. Nadykto, F. Yu, L. Jiang and W. Wang, *J. Mol. Struct.: THEOCHEM.*, 2010, **951**, 28-33.

34. Y.-P. Zhu, Y.-R. Liu, T. Huang, S. Jiang, K.-M. Xu, H. Wen, W.-J. Zhang and W. Huang, *J. Phys. Chem. A*, 2014, **118**, 7959-7974.

35. J. Kim, H. M. Lee, S. B. Suh, D. Majumdar and K. S. Kim, *J. Chem. Phys.*, 2000, **113**, 5259-5272.

36. B. Delley, *J. Chem. Phys.*, 1990, **92**, 508-517.

37. W. Huang, A. P. Sergeeva, H.-J. Zhai, B. B. Averkiev, L.-S. Wang and A. I. Boldyrev, *Nat. Chem.*, 2010, **2**, 202-206.

38. W. Huang, H.-J. Zhai and L.-S. Wang, *J. Am. Chem. Soc.*, 2010, **132**, 4344-4351.

39. Y.-R. Liu, H. Wen, T. Huang, X.-X. Lin, Y.-B. Gai, C.-J. Hu, W.-J. Zhang and W. Huang, *J. Phys. Chem. A*, 2014, **118**, 508-516.

40. K.-M. Xu, T. Huang, H. Wen, Y.-R. Liu, Y.-B. Gai, W.-J. Zhang and W. Huang, *RSC Adv.*, 2013, **3**, 24492-24502.

41. H. Wen, Y.-R. Liu, K.-M. Xu, T. Huang, C.-J. Hu, W.-J. Zhang and W. Huang, *RSC Adv.*, 2014, **4**, 15066-15076.

42. X.-X. Lin, Y.-R. Liu, T. Huang, K.-M. Xu, Y. Zhang, S. Jiang, Y.-B. Gai, W.-J. Zhang and W. Huang, *RSC Adv.*, 2014, **4**, 28490-28498.

43. C. Romanescu, A. P. Sergeeva, W.-L. Li, A. I. Boldyrev and L.-S. Wang, *J. Am. Chem. Soc.*, 2011, **133**, 8646-8653.

44. K. H. Weber, F. J. Morales and F.-M. Tao, *J. Phys. Chem. A*, 2012, **116**, 11601-11617.

45. Y. Xu, A. B. Nadykto, F. Yu, J. Herb and W. Wang, *J. Phys. Chem. A*, 2009, **114**, 387-396.

46. J. Herb, A. B. Nadykto and F. Yu, *Chem. Phys. Lett.*, 2011, **518**, 7-14.

47. T. L. Fonseca, M. A. Castro, B. J. Cabral, K. Coutinho and S. Canuto, *Chem. Phys. Lett.*, 2009, **481**, 73-77.

48. J. Elm, P. Norman, M. Bilde and K. V. Mikkelsen, *Phys. Chem. Chem. Phys.*, 2014, **16**, 10883-10890.

49. S. Jiang, T. Huang, Y.-R. Liu, K.-M. Xu, Y. Zhang, Y.-Z. Lv and W. Huang, *Phys. Chem. Chem. Phys.*, 2014, **16**, 19241-19249.

50. X.-Q. Peng, Y.-R. Liu, T. Huang, S. Jiang and W. Huang, *Phys. Chem. Chem. Phys.*, 2015, **17**, 9552-9563.

51. H. Forbert, M. Masia, A. Kaczmarek-Kedziera, N. N. Nair and D. Marx, *J. Am. Chem. Soc.*, 2011, **133**, 4062-4072.

52. A. Gutberlet, G. Schwaab, Ö. Birer, M. Masia, A. Kaczmarek, H. Forbert, M. Havenith and D. Marx, *Science*, 2009, **324**, 1545-1548.

53. K. R. Leopold, *Annu. Rev. Phys. Chem.*, 2011, **62**, 327-349.

54. W. H. Robertson and M. A. Johnson, *Science*, 2002, **298**, 69-69.

55. B. Temelso, T. N. Phan and G. C. Shields, *J. Phys. Chem. A*, 2012, **116**, 9745-9758.

56. B. Temelso, T. E. Morrell, R. M. Shields, M. A. Allodi, E. K. Wood, K. N. Kirschner, T. C. Castonguay, K. A. Archer and G. C. Shields, *J. Phys. Chem. A*, 2012, **116**, 2209-2224.

57. J. Kim, B. J. Mhin, S. J. Lee and K. S. Kim, *Chem. Phys. Lett.*, 1994, **219**, 243-246.

58. B. J. Mhin, S. J. Lee and K. S. Kim, *Phys. Rev. A*, 1993, **48**, 3764.

59. H. M. Lee, S. B. Suh, J. Y. Lee, P. Tarakeshwar and K. S. Kim, *J. Chem. Phys.*, 2000, **112**, 9759-9772.

60. J. C. Ianni and A. R. Bandy, *J. Phys. Chem. A*, 1999, **103**, 2801-2811.

61. L. Torpo, T. Kurten, H. Vehkamäki, K. Laasonen, M. R. Sundberg and M. Kulmala, *J. Phys. Chem. A*, 2007, **111**, 10671-10674.

62. Z.-L. Lv, K. Xu, Y. Cheng, X.-R. Chen and L.-C. Cai, *J. Chem. Phys.*, 2014, **141**, 054309.

63. V. Loukonen, T. Kurtén, I. Ortega, H. Vehkamäki, A. A. Padua, K. Sellegri and M. Kulmala, *Atmos. Chem. Phys.*, 2010, **10**, 4961-4974.

64. M. Noppel, H. Vehkamäki and M. Kulmala, *J. Chem. Phys.*, 2002, **116**, 218-228.

65. D. Bustos, B. Temelso and G. C. Shields, *J. Phys. Chem. A*, 2014, **118**, 7430-7441.

66. E. Orestes, P. Chaudhuri and S. Canuto, *Mol. Phys.*, 2012, **110**, 297-306.

67. T. K. Ghanty and S. K. Ghosh, *J. Chem. Phys.,* 2003, **118**, 8547-8550.

Table 1. Boltzmann Averaged Binding Energies of OA-SA-W$_n$.[a]

n	ΔE (0 K)	ΔH (298.15 K)	ΔG (298.15 K)
0	-15.01	-14.82	-5.38
1	-10.70	-11.50	-1.98
2	-10.28	-11.31	-1.50
3	-11.12	-12.27	-0.97
4	-11.16	-12.37	-0.60
5	-8.77	-9.58	-0.62
6	-9.78	-10.36	-0.94

[a] Boltzmann averaged binding energies in kcal mol^{-1} at the PW91PW91 /6-311++G(3df,3pd) level of OA-SA-W$_n$(n=0-6) in the reaction OA + SA $\rightarrow$ OA-SA or OA-SA-W$_{n-1}$ + W $\rightarrow$ OA-SA-W$_n$(n=1-6).

Figure Captions

Figure 1. Optimized geometries of OA-SA-W_n(n=0-6) at the PW91PW91/6-311++G

(3df,3pd) level.

Figure 2. Thermodynamics at the PW91PW91/6-311++G(3df,3pd) level of stepwise

sulfuric acid-oxalic acid dimer hydrate growth of the neutral (N), di-ionic

OA-SA$^-$-W$^+$-W_{n-1} (SA), di-ionic OA$^-$-SA-W$^+$-W_{n-1} (OA), tetra-ionic OA$^-$-SA$^-$-(W$^+$)$_2$-

W_{n-2} (SA&OA). The change in energy is defined as the difference between the

Boltzmann averaged value for the nth of a particular state (N, SA, OA, SA&OA) and

the (n−1)th cluster of all states.

Figure 3. The conformational population changes for the low-energy isomers of

OA-SA-W_n(n=1 - 6) over a temperature range of 100 to 400 K.

Figure 4. Boltzmann averaged Gibbs free energy at the PW91PW91

/6-311++G(3df,3pd) level of stepwise sulfuric acid-oxalic acid dimer hydrate growth

over a temperature range of 100 to 400 K.

Figure 5. Hydrate distributions of clusters with sulfuric acid-oxalic acid (SA-OA)

dimers at four different relative humidities (RH = 20%, 50%, 80% and 100%).

Figure 6. The Rayleigh light scattering and cluster polarizability properties: (a)

isotropic mean polarizabilities as a function of water molecules; (b) anisotropic

polarizabilities as a function of water molecules; (c) Rayleigh light scattering

intensities as the function of water molecules; (d) depolarization ratio as a function of
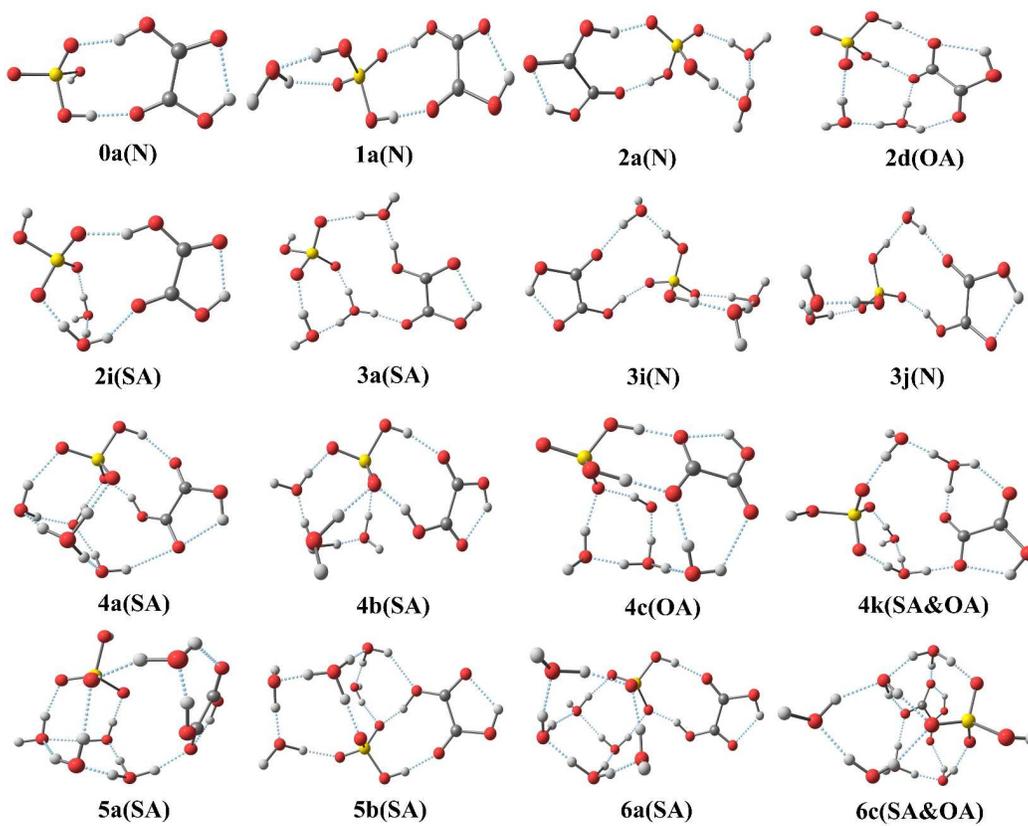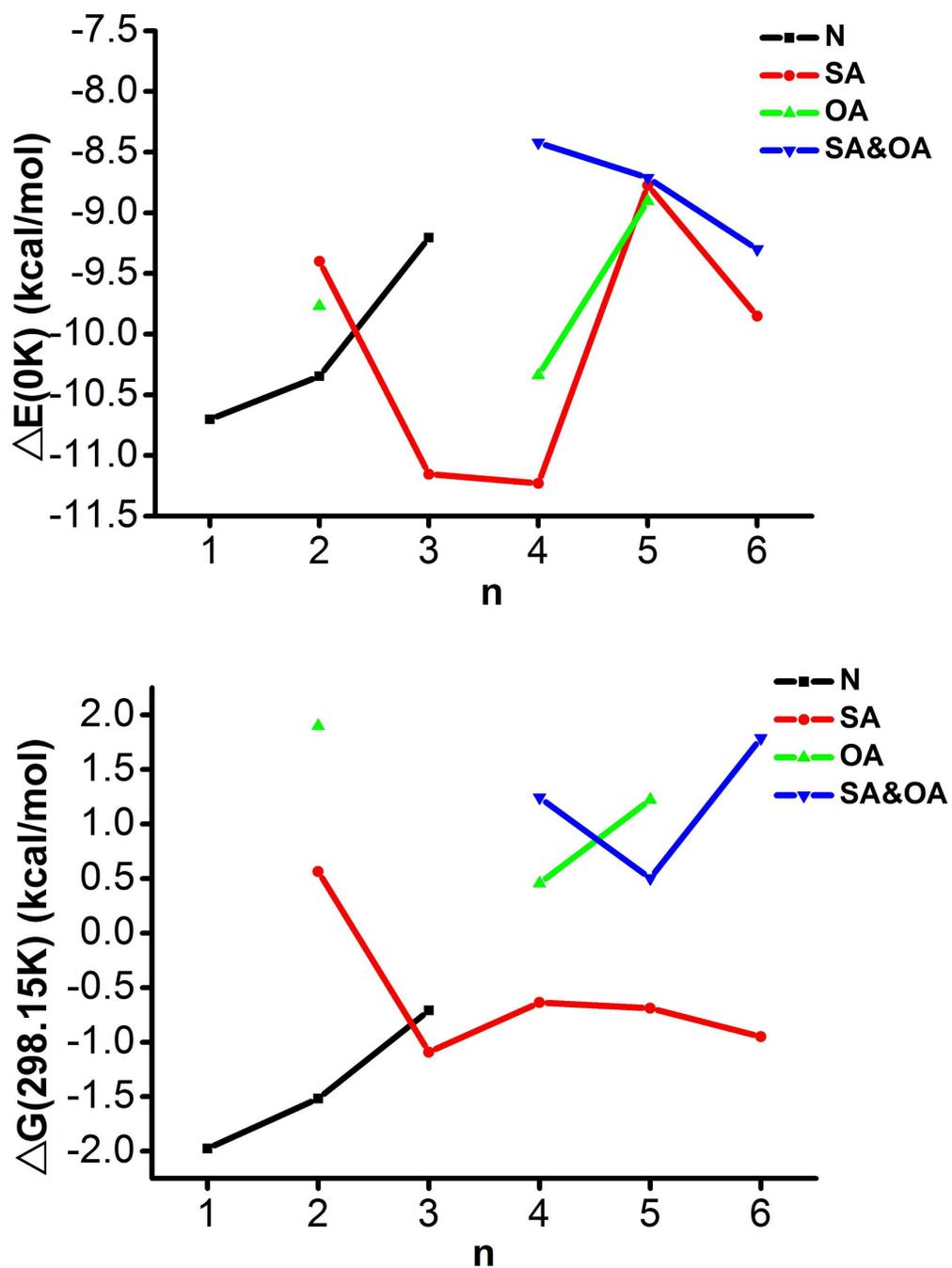
water molecule.

Figure 1.

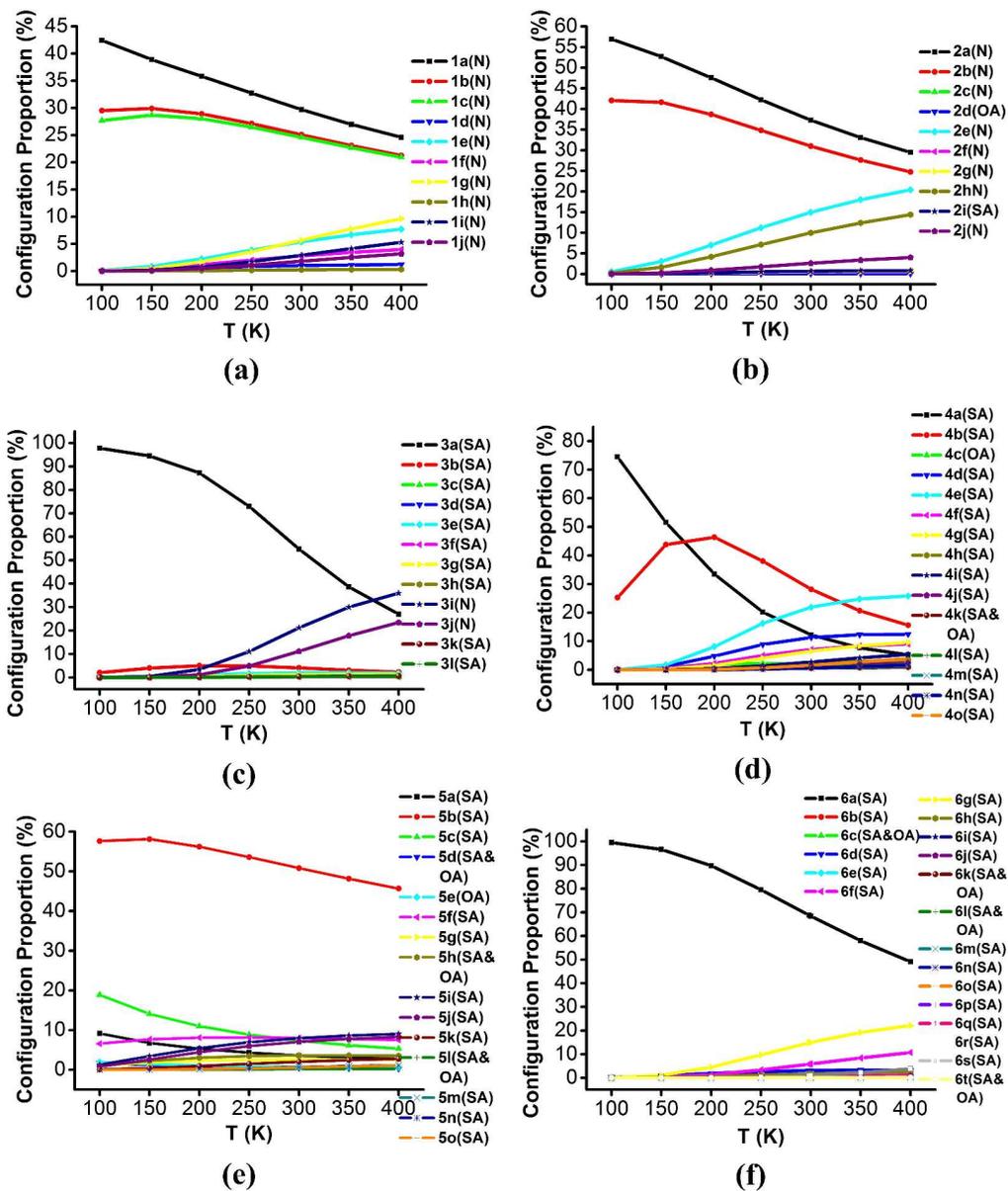0a(N) 1a(N) 2a(N) 2d(OA)

2i(SA) 3a(SA) 3i(N) 3j(N)

4a(SA) 4b(SA) 4c(OA) 4k(SA&OA)

5a(SA) 5b(SA) 6a(SA) 6c(SA&OA)

Figure 2.

Figure 3.

Figure 4.

Figure 5.

Figure 6.

(a)

(b)

(c)

(d)

28